RNAL OF VIROLOGY, May 1996, p. 2982–2991
0022-538X/96/$04.00+0

Vol. 70, No. 5

Biophysical Characterization of Recombinant Proteins Expressing the Leucine Zipper-Like Domain of the Human Immunodeficiency Virus Type 1 Transmembrane Protein gp41

DIANE C. SHUGARS, CARL T. WILD, TERESA K. GREENWELL, AND THOMAS J. MATTHEWS*
Department of Surgery, Duke University Medical Center, Durham, North Carolina 27710

Received 6 June 1995/Accepted 26 January 1996

Envelope oligomerization is thought to serve several crucial functions during the life cycle of human immunodeficiency virus type 1 (HIV-1). We recently reported that virus entry requires coiled-coil formation of the leucine zipper-like domain of the HIV-1 transmembrane envelope glycoprotein gp41 (C. Wild, T. Oas, C. McDanal, D. Bolognesi, and T. Matthews, Proc. Natl. Acad. Sci. USA 89:10537–10541, 1992; C. Wild, J. W. Dubay, T. Greenwell, T. Baird, Jr., T. G. Oas, C. McDanal, E. Hunter, and T. Matthews, Proc. Natl. Acad. Sci. USA 91:12676–12680, 1994). To determine the oligomeric state mediated by this region of the envelope, we have expressed the zipper motif as a fusion partner with the monomeric maltose-binding protein of *Escherichia coli*. The biophysical properties of this protein were characterized by velocity and equilibrium sedimentation, size exclusion chromatography, light scattering, and chemical cross-linking analyses. Results indicate that the leucine zipper sequence from HIV-1 is capable of multimerizing much larger and otherwise monomeric proteins into extremely stable tetramers. Recombinant proteins containing an alanine or a serine substitution at a critical isoleucine residue within the zipper region were also generated and similarly analyzed. The alanine- and serine-substituted proteins behaved as tetrameric and monomeric species, respectively, consistent with the influence of these same substitutions on the helical coiled-coil structure of synthetic peptide models. On the basis of these findings, we propose that the fusogenic gp41 structure involves tetramerization of the leucine zipper domain which is situated approximately 30 residues from the N-terminal fusion peptide sequence.

Envelope multimerization is thought to be critical for replication of fusogenic viruses such as human immunodeficiency virus type 1 (HIV-1) (for reviews, see references 17, 40, and 50). Oligomerization of the viral envelope (Env) polypeptide precursor gp160 is required for the processing and intracellular transport (16, 17, 21) of a functional Env complex (composed of the surface glycoprotein gp120 and the transmembrane protein gp41). This process has been termed assembly oligomerization and is mediated through gp41 (19, 20). On the surfaces of virus particles and infected cells, gp120 and gp41 are found noncovalently associated in multimeric Env complexes that have been variously described as dimers (19, 39, 49), trimers (25, 35, 37), and tetramers (19, 37, 39, 40, 45, 49). Virus entry also requires multimerization of the leucine zipper-like domain (15) of gp41 via an intact coiled-coil structure (10, 11, 18, 51, 52), a process recently referred to as fusogenic oligomerization (51).

While the molecular determinants of the different types of Env oligomerization have been defined to various degrees, the unique nature of the gp41 leucine zipper-like motif allows for a more rigorous characterization. First described for eukaryotic transcriptional activators (28), the leucine zipper consists of four or five heptad repeat units of hydrophobic (typically leucine or isoleucine) residues located at the first and fourth positions of each heptad. The heptad motif gives rise to α-helices that have been predicted to specifically associate along a hydrophobic interface to form a coiled-coil structure (12, 13). This structural prediction has been confirmed by X-ray crystallographic studies (23, 33) using synthetic peptides that accurately model the leucine zipper of the yeast transcription factor GCN4. On the basis of secondary structural analyses, Gallaher and colleagues (24) identified a 33-residue region (residues 560 to 592 of HIV-1_{AI} gp160; numbering according to reference 31) of gp41 that was predicted to assume an extended amphipathic α-helix. This region was later shown to contain several characteristics of the classic leucine zipper (15). We have modeled this region using the synthetic peptide DP-107 (residues 558 to 595 of gp160) and have shown that this region does indeed exhibit structural components characteristic of a coiled coil (51, 52). The gp41 zipper motif is highly conserved among isolates of HIV-1, HIV-2, and the related simian immunodeficiency viruses (15, 31). Similar heptad repeat sequences have also been detected in the transmembrane envelope proteins of other families of viruses such as influenza viruses (8), paramyxoviruses (4, 5, 8), and coronaviruses (3, 8), pointing to a conserved functional role for this region in virus replication.

Since leucine zippers have been shown to mediate dimerization of several DNA-binding transcription factors (28, 34), it has been suggested that the zipper domain of gp41 may be responsible for multimerization of HIV-1 Env (15, 24). The assembly domain of gp160 has been mapped to a 62-residue region (residues 584 to 646 of gp160) located within the extracellular domain of gp41 and overlaps the last heptad repeat unit of the zipper-like motif (20). However, direct involvement of this latter motif in Env assembly oligomerization has yet to be demonstrated. In contrast, oligomerization of the gp41 zipper domain has been shown to be critical for Env multimerization during the virus entry process (10, 11, 18, 51, 52). In synthetic peptide models evaluated by circular dichroism (51, 52), single helix-disrupting nonconservative substitutions (e.g., proline or serine) at an invariant isoleucine residue (position 578) centrally located in the gp41 zipper sequence abrogated coiled-coil formation, unlike the case for peptides containing a

* Corresponding author. Mailing address: Department of Surgery, Duke University Medical Center, Campus Box 2926, Durham, NC 27710. Phone: (919) 684-4215. Fax: (919) 684-4288.

Exhibit A

conservative substitution (e.g., alanine) at that position. Furthermore, the ability of these peptides to assume a coiled-coil structure was directly related to their antiviral activity (51, 52). HIV-1 Env glycoproteins containing the same nonconservative substitutions failed to mediate cell fusion when evaluated in an Env expression system, although the synthesis, processing, assembly oligomerization, and cell surface expression of the Env complexes were unaltered (11, 18, 51). In addition, viruses containing nonconservative substitutions at that position were unable to undergo membrane fusion and consequently failed to initiate an infection (11, 18). In related studies by Chen and colleagues (10, 11), single proline substitutions at four critical isoleucine or leucine residues within the zipper motif yielded similar results. These collective findings have led to the hypothesis that the coiled-coil structure of the gp41 leucine zipper motif is involved in the formation of the fusogenic oligomer but not the native prefusogenic oligomer. Such a model then is reminiscent of the structural transition of an analogous sequence in the influenza virus hemagglutinin envelope glycoprotein membrane protein (HA2) that occurs during pH-induced membrane fusion, as described recently by Carr and Kim (7) and by Bullough et al. (6).

Traditionally synthetic peptides have been used to model coiled-coil structures in biological systems (34). Despite numerous attempts, we have been unable to determine the exact oligomeric state (e.g., dimer, trimer, or tetramer) of the gp41 leucine zipper region via sedimentation analysis of DP-107 and related synthetic peptides. As an alternative approach, we have expressed this domain as a fusion partner with the monomeric maltose-binding protein (MBP) of *Escherichia coli* (2). This strategy allows for a more rigorous biophysical characterization, as coiled-coil formation in this context would require multimerization of a much larger heterologous protein. To assess the influence of single substitutions at residue 578 on protein oligomerization, mutant recombinant proteins containing either an alanine or a serine substitution at this position were also generated. The physical properties of the recombinant proteins were characterized by five well-established methods: sedimentation velocity and equilibrium ultracentrifugation, size exclusion chromatography, light scattering, and chemical cross-linking. The biological properties of these proteins were also evaluated in an assay for virus-mediated cell fusion. In these studies, the recombinant proteins appeared to accurately model the gp41 coiled-coil structure. Using these complementary approaches, we determine the multimeric valency of this region as expressed as a recombinant protein and evaluate the effects of residue substitutions on polypeptide oligomerization. Finally, we discuss potential roles that the gp41 zipper may assume in the virus entry process.

MATERIALS AND METHODS

Plasmid construction. A fragment of the HIV-1$_{HXB2}$ *env* gene (nucleotides 2110 to 2256 [14]) encoding amino acids 550 to 598 of gp160 was generated via PCR amplification of plasmid pgTAT (30). After purification, the fragment was cloned into the pMAL-p2 vector (New England Biolabs, Beverly, Mass.) at the *Xmn*I and *Eco*RI sites, in frame with the *malE* gene, which encodes MBP (26). DNAs encoding the fusion proteins MBPAla and MBPSer were generated by PCR-directed mutagenesis of pgTAT, using overlapping amplification primers (27) which change the ATC codon specifying an isoleucine residue at position 578 to GCC (alanine) and TCC (serine), respectively. All 3′ amplification primers introduce a stop codon immediately following the gp41 coding sequence. To generate DNA expressing the control protein MBPstop, an *Nhe*I linker (5′-GGCTAGCC-3′; New England Biolabs) encoding a stop codon was introduced into the *Xmn*I site of pMAL-p2 immediately downstream of the *malE* coding sequence. Use of this linker resulted in the addition of a glycine residue to the C terminus of the plasmid-encoded carrier sequence. All insert sequences were confirmed by dideoxy sequencing using Sequenase enzyme (Amersham/Life Sciences, Arlington Heights, Ill.).

Protein expression and purification. Fusion proteins were expressed at 37°C in *E. coli* NovaBlue cells (*endA1 hsdR17* (r_{K12}^- m_{K12}^+) *supE44 thi-1 recA1 gyrA96 relA1 lac* [F′ *proA*$^+$*B*$^+$ *lacI*^{q}*ZΔM15::Tn10*(Tet^r)]; Novagen, Madison, Wis.). Following induction with isopropylthiogalactoside (IPTG), proteins were extracted from the bacterial periplasmic space via osmotic shock treatment and purified by amylose affinity chromatography as recommended by the manufacturer. Protease inhibitors (aprotonin at 2 μg/ml, phenylmethylsulfonyl fluoride at 40 μg/ml, pepstatin A at 1 μg/ml, and leupeptin at 2 μg/ml; all obtained from Sigma, St. Louis, Mo.) were added during purification. Protein-containing fractions were pooled, dialyzed against phosphate-buffered saline (PBS; 137 mM NaCl, 2.7 mM KCl, 1.5 mM KH_2PO_4, 6.5 mM Na_2HPO_4, [pH 7.4]), and concentrated by lyophilization, and the reconstituted proteins were stored at −70°C prior to analysis. Typical yields ranged from 4 to 6 mg/liter of culture.

Peptide synthesis. Peptides were synthesized on an Applied Biosystems model 431A peptide synthesizer by using Fast Moc chemistry and purified by reverse-phase high-pressure liquid chromatography as described previously (52). The molecular masses of the peptides were confirmed by electrospray mass spectrometry. Peptide and protein concentrations were determined spectrophotometrically at A_{280} (22).

Analytical ultracentrifugation. Sedimentation velocity and equilibrium analyses were performed, using a Beckman Optima XL-A analytical ultracentrifuge equipped with absorbance optics and an An-60Ti rotor (Beckman Instruments Inc., Palo Alto, Calif.). For velocity studies, proteins were evaluated at concentrations ranging from 0.3 to 1.2 mg/ml in PBS. Samples were placed in two-channel Epon centerpieces and centrifuged at 3,000 rpm and 25°C to confirm initial solute concentrations. Samples were then subjected to velocity centrifugation for 4 h at 24,000 rpm. Radial distributions of proteins were monitored by optical absorbance at 280 nm, and boundary sedimentation data were collected at 15-min intervals. Data from 7 to 10 consecutive scans were analyzed to determine an apparent weight average sedimentation coefficient (s) for each protein. Raw s values were derived by the transport method (44) and corrected to standard conditions ($s_{20,w}$) by using partial specific volumes (v, determined from the amino acid composition and adjusted for temperature), solvent density (ρ), and solvent viscosity as previously described (29). Estimated molecular weights (M) were determined from corrected s coefficients by using the formula

$$M^{20} = \frac{\bar{s}^{20}}{0.01(1 - \bar{v}\rho)}.$$

Sedimentation equilibrium analyses of MBP107 in six-channel Epon centerpieces were conducted at 20°C and at four (for 1.5, 0.75, and 0.38 mg/ml in PBS) or five (for 0.14 mg/ml in PBS) rotor speeds that ranged from 7,000 to 12,000 rpm. Radial distributions of proteins were monitored by optical absorbance at 280 or 220 nm, and data (approximately 100 datum points at each concentration and rotor speed) were collected after equilibrium had been established, as judged from superimposition of successive scans taken at least 3 h apart. Using the Optima XL-A Data Analysis software program, sedimentation equilibrium data were fitted to theoretical curves predicted for each of four models for evaluation of single data sets. These models employ a nonlinear least-squares fit algorithm to model the following species: (i) a single ideal species, (ii) a single nonideal species, (iii) two noninteracting species, and (iv) a reversible associating system represented by up to four species. Multiple data sets were analyzed simultaneously, using the multi-scif model. The theoretical monomeric molecular size of MBP107 (48,184 Da) served as the basis for molecular weight considerations in the self-associating monomer-multimer models.

Size exclusion chromatography. Proteins were also evaluated by gel filtration fast protein liquid chromatography (FPLC). Sample aliquots were injected onto a Superdex 200 column (1 by 30 cm diameter; Pharmacia Biotec, Piscataway, N.J.) equilibrated with 250 mM sodium phosphate buffer (pH 7.1) containing 125 mM NaCl at room temperature. The flow rate was 0.5 ml/min, and absorbance was monitored at 214 nm. The following globular protein standards were obtained from Sigma Chemical Company: β-amylase (200 kDa), alcohol dehydrogenase (150 kDa), bovine serum albumin (66 kDa), and carbonic anhydrase (29 kDa). Also used as protein standards were murine immunoglobulin G2b (150 kDa) and human gamma globulin fraction II (156 kDa). Apparent molecular weights of the fusion proteins were determined by comparing their elution peaks (calculated as the ratio of elution volume [V_e] to void volume [V_o]) against a calibration curve generated by the elution peaks of the protein standards. V_o was determined by gel filtration of blue dextran.

Light scattering. Light scattering analyses (36) were conducted with a DynaPro-801 instrument (Protein Solutions, Charlottesville, Va.). Samples (1 mg/ml in PBS) were centrifuged briefly, and the supernatants were passed through either a 0.02- or 0.01-μm-pore-size filter prior to analysis. Three to five independent determinations at room temperature were made for each sample. The apparent molecular weight of each sample was determined from the measured translational diffusion coefficient and hydrodynamic radius by using the DynaPro-801 AutoPro software program. Light scattering data were best fitted either to a monomodal regression model (for samples containing a single component) or to a bimodal regression model (for samples containing two components).

Chemical cross-linking. MBP107 was further analyzed following chemical cross-linking with ethylene glycol bis(succinimidyl succinate) (EGS; Sigma). Freshly

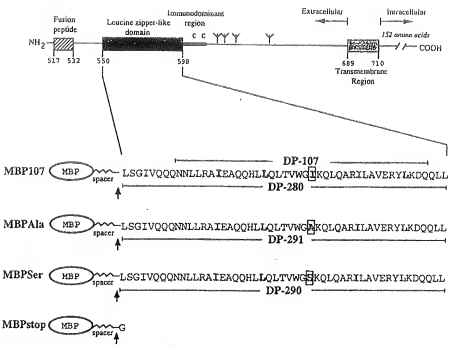

FIG. 1. Diagram of MBP-based recombinant proteins expressing the HIV-1 gp41 leucine zipper-like domain. The HIV-1 gp41 transmembrane glycoprotein is shown as a linear schematic. Highlighted is the 49-residue region (residues 550 to 598 of HIV-1_{LAI} gp160) present in the recombinant proteins. The leucine and isoleucine residues of the heptad repeat units are indicated by outline type. Residues corresponding to synthetic peptides used in this study are depicted relative to the protein sequences. The factor Xa cleavage site is marked by an arrow, and residue position 578 is boxed.

prepared EGS dissolved in dimethyl sulfoxide was added to MBP107 (~0.5 mg/ml), and *N*-2-hydroxyethylpiperazine-*N*′-2-ethanesulfonic acid (HEPES; pH 7.5) was added to a final concentration of 100 mM. The final EGS concentrations are indicated in the legend to Fig. 6. After a 1-h incubation on ice, the reactions were quenched for 30 min with glycine (100 mM [final concentration], pH 7.0). The protein was then treated with sodium dodecyl sulfate (SDS) disruption buffer and dialyzed against Tris-SDS buffer (50 mM Tris-HCl [pH 6.8], 1% SDS) overnight at 4°C before analyzing by SDS-polyacrylamide gel electrophoresis (PAGE).

Cells and virus. CEM cells (obtained from P. Cresswell, Duke University Medical Center, Durham, N.C.) were propagated in RPMI 1640 culture medium containing 10% fetal calf serum. Molt-4 cells (obtained from J. Hoxie, University of Pennsylvania, Philadelphia, Pa.) were cultured in RPMI 1640 medium containing 20% fetal calf serum. $HIV\text{-}1_{IIIB}$ was originally obtained from R. Gallo (National Cancer Institute, Bethesda, Md.) (38).

HIV-1 cell fusion assay. The ability of fusion proteins and peptides to inhibit virus-mediated cell fusion was evaluated as described previously (52). In a 96-well microtiter plate format, CEM cells (10^5 in 45 μl of culture medium) chronically infected with $HIV\text{-}1_{IIIB}$ were incubated with uninfected Molt-4 cells (7×10^5 in 45 μl of culture medium) in the presence or absence of inhibitor (10 μl, twofold concentrations in PBS). After a 24-h incubation at 37°C, multinucleated giant cells (syncytia) present in the cell culture were enumerated by microscopic examination.

RESULTS

Construction, expression, and purification of fusion proteins. To evaluate the oligomeric properties of the gp41 leucine zipper-like domain in the context of a protein, this region was expressed as a fragment fused to the C terminus of the *E. coli* MBP. As diagrammed in Fig. 1, the leucine zipper region lies within the extracellular domain of gp41 and is located approximately 30 residues C terminal to the fusion peptide domain in the linear gp41 amino acid sequence.

The recombinant protein MBP107 contains a total of 436 residues: 387 residues encoded by pMAL-p2 and 49 residues derived from gp41 (Fig. 1). The pMAL-p2 vector encodes MBP (373 residues) followed by a 10-glutamine residue spacer and the four-residue factor Xa digestion site (Ile-Glu-Gly-Arg). The gp41-derived region includes 38 residues modeled by the peptide DP-107 (50) and an additional 8 residues N terminal and 3 residues C terminal to the DP-107 region. The additional N-terminal residues lengthen the plasmid-encoded spacer located between the MBP- and gp41-specific sequences, thus permitting the fusion proteins greater flexibility to bind to the amylose resin during affinity purification and potentially enabling the gp41-derived region to adopt an intermolecular coiled-coil structure. The protease factor Xa cleavage site allows the gp41-derived polypeptide to be separated from the MBP fusion partner following factor Xa digestion (32). As estimated by SDS-PAGE (Fig. 2), MBP107 migrates with a molecular mass of approximately 50 kDa, consistent with its calculated molecular mass of 48.2 kDa.

Also constructed were DNAs expressing mutant proteins that contain a single substitution of either alanine (MBPAla) or serine (MBPSer) at an isoleucine residue (I-578) centrally located within the coiled coil (Fig. 1). Single point mutations at this position have been shown to alter the biophysical properties of the gp41 coiled coil when modeled as peptides (51, 52). MBPAla and MBPSer also have apparent molecular masses of approximately 50 kDa in SDS-PAGE (Fig. 2). As a control, DNA encoding only the MBP carrier was generated. The resultant protein MBPstop encodes 388 residues (387 MBP-

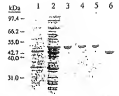

FIG. 2. Expression of recombinant proteins. Proteins were expressed in *E. coli* following induction with IPTG and were subjected to SDS-PAGE (10% gel). Shown are preinduction (lane 1), postinduction (lane 2), and affinity-purified (lane 3) samples of MBP107. Also shown are affinity-purified MBPAla (lane 4), MBPSer (lane 5), and MBPstop (lane 6). Positions of molecular weight markers are shown on the left.

derived residues and a C-terminal glycine residue generated during plasmid construction). Its apparent molecular mass of 44 kDa (Fig. 2) is also consistent with the theoretical molecular mass of 42.6 kDa.

Fusion proteins were overexpressed in bacterial cells following IPTG induction. The presence of an export signal encoded by *malE* enabled the proteins to be exported into the periplasmic space, a process thought to promote the native folding of bacterially expressed proteins (48). One-step affinity chromatography was used to purify the fusion proteins to ≥95% homogeneity as assessed by SDS-PAGE followed by Coomassie blue staining (Fig. 2).

Analysis by velocity sedimentation. Recombinant proteins were subjected to velocity analytical centrifugation as an initial attempt to determine the oligomeric state of the gp41 zipper domain. In three independent experiments, various concentrations of the recombinant proteins (0.3 to 1.2 mg/ml in PBS) were analyzed at 25°C and 24,000 rpm. Representative sedimentation scans are shown in Fig. 3. Apparent molecular weights were estimated from the normalized s coefficients and compared with the theoretical monomeric molecular weights (Table 1).

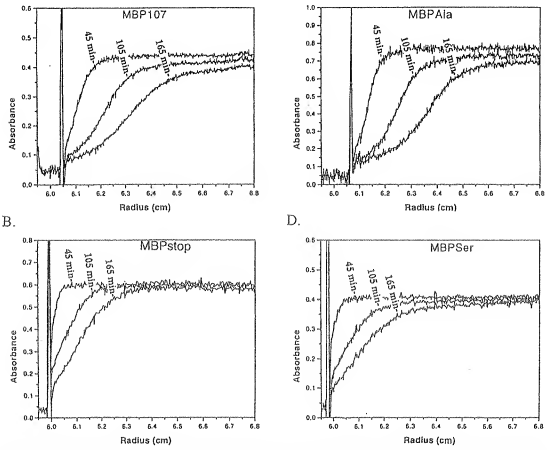

FIG. 3. Velocity sedimentation ultracentrifugation of recombinant proteins. Proteins (0.4 to 0.8 mg/ml in PBS) were centrifuged in an Optima XL-A centrifuge at 24,000 rpm and 25°C, and boundary sedimentation data were collected at 15-min intervals. Shown are raw data from scans taken at 45-, 105-, and 165-min intervals, plotted as the absorbance of the solute concentration at 280 nm versus the radial distance. The peak located at the left of each scan marks the sample meniscus. Sedimentation is from left to right.

TABLE 1. Sedimentation velocity measurements of recombinant proteins

Protein	Sedimentation coefficient[a] (S)	Apparent avg mol wt ± SD	Ratio, apparent mol wt/monomer mol wt[b]
MBP107	9.3–9.5	191,610 ± 3,335	4.0
MBPstop	3.3–4.0	47,120 ± 4,620	1.1
MBPAla	9.0–10.3	204,470 ± 22,430	4.2
MBPSer	4.0–4.4	59,320 ± 5,220	1.2

[a] Obtained for each protein from three independent determinations (24,000 rpm and 25°C) and were standardized to $s_{20,w}$. The range of estimates is shown.
[b] Molecular weight in solution compared with the theoretical monomer molecular weight.

In these studies, MBP107 consistently sedimented at a faster rate than MBPstop (compare Fig. 3A and B). The s coefficients for MBP107 ranged from 9.3 to 9.5 and corresponded to an average estimated molecular size of 191,600 Da, indicative of a tetrameric species (Table 1). In contrast, velocity sedimentation of MBPstop resulted in an average s coefficient of 3.6 and a corresponding apparent molecular size of 47,100 Da. Thus, MBPstop sedimented as a monomer as has been previously described (2). Similar results were obtained from velocity studies conducted at 32,000 rpm and at 20°C (data not shown). Velocity sedimentation of MBP107 in the presence of maltose did not alter its sedimentation rate (data not shown), indicating that protein multimerization occurs through the gp41-derived region rather than the MBP carrier.

To determine the effects of single helix-disrupting (e.g., serine) and non-helix-disrupting (e.g., alanine) mutations in the coiled-coil region on gp41 multimerization, recombinant proteins containing an alanine (MBPAla) or serine (MBPSer) substitution at position 578 were also examined by velocity sedimentation. Representative sedimentation scans of MBPAla and MBPSer are shown in Fig. 3C and D, and results from three experiments are summarized in Table 1. MBPAla sedimented with s values that corresponded to a tetrameric form, while MBPSer sedimented with s values that approximated those of a monomeric species. Therefore, the oligomeric states of these mutant proteins are consistent with the ability of these single residue changes to affect coiled-coil formation, as has been reported for synthetic peptide models (51, 52).

Analysis by sedimentation equilibrium ultracentrifugation. While the results from sedimentation velocity experiments were suggestive of a tetrameric form for MBP107, this fusion protein was further evaluated by the more accurate sedimentation equilibrium method. Data collected at multiple protein concentrations and rotor speeds were fitted initially to several models to identify the one that best described the sedimenting species. Results from these analyses indicated that the self-associating monomer-tetramer model best described the behavior of MBP107, as determined by the observed fits to the theoretical monomer-tetramer curves (χ^2 values ranged from 1.3×10^{-4} to 4.1×10^{-5}) and the random distributions of the fit residuals. As a representative example, Fig. 4 depicts the results of fitting the data generated by analysis of MBP107 at 1.5 mg/ml (7,000 rpm at 20°C) to self-associating monomer-dimer, -trimer, -tetramer, and -dimer-tetramer models. Simultaneous fitting of multiple data sets obtained from analysis of MBP107 at 0.14 mg/ml and five rotor speeds (7,000 to 12,000 rpm) also confirmed the best fit of the monomer-tetramer model (global goodness of fit = 0.5663 and randomly distributed fit residuals; data not shown). For comparison, MBPstop (0.75 mg/ml) was also subjected to equilibrium sedimentation analysis under similar conditions (10,000 rpm at 20°C). Data were best fitted to those for a single ideal species having a calculated molecular weight of 42,544 ($\chi^2 = 3.39 \times 10^{-5}$; data not shown), in excellent agreement with its theoretical molecular weight of 42,600.

To determine the relative concentrations of the monomeric and tetrameric components of MBP107, monomer-tetramer association constants ($K_{a1,4}$) were determined from the absorbance constants obtained at each protein concentration and rotor speed (43). The large $K_{a1,4}$ values (approximately 10^{16} M^{-3}; data not shown) and tetramer-to-monomer concentrations (~8,000:1; data not shown) argue that MBP107 exists almost entirely as a tetrameric species, with very little detectable monomeric component. The uniform, symmetrical boundary fronts generated from successive scans of MBP107 during velocity sedimentation (Fig. 3A) also point to a discrete oligomeric species assumed by this protein in solution. No evidence of an intermediate dimeric state was observed, since data fitting to a monomer-dimer-tetramer model was no better than the theoretical fit to the monomer-tetramer model (Fig. 4C and D).

Analysis of fusion proteins by size exclusion chromatography. The recombinant proteins were also evaluated by size exclusion chromatography to confirm their multimeric states. Apparent molecular weights of the recombinant proteins were estimated by comparing their elution volumes with those of well-characterized protein standards. Data obtained from four independent determinations for each protein are presented as averaged values in Fig. 5.

In these studies, MBP107 eluted as a peak with an average molecular mass of 187 kDa (range, 175 to 209 kDa). This apparent molecular mass closely approximates that of a tetramer having a theoretical molecular mass of 192.6 kDa. To confirm that the elution peak of MBP107 does indeed represent an oligomeric form, fractions from chromatographed MBP107 were collected and analyzed by SDS-PAGE (10% gel). Single protein bands of approximately 50 kDa were observed in fractions containing the elution peak (data not shown). Rechromatographing of the peak MBP107 elution fraction after storage for 24 h at 4°C revealed only a single tetrameric form (data not shown), confirming the stability of this protein as an oligomer. In contrast, MBPstop eluted as a single peak with an average molecular mass of 41 kDa (range, 40 to 43 kDa), consistent with the monomeric state of this protein (2).

The mutant fusion proteins were similarly analyzed by FPLC. The elution peak for MBPAla corresponded to an average molecular mass of 217 kDa (range, 209 to 222 kDa), while its serine-substituted counterpart MBPSer eluted as a single peak with apparent average molecular mass of 45 kDa (range, 44 to 49 kDa). Thus, MBPAla and MBPSer behave as oligomeric and monomeric species, respectively, consistent with results obtained from analytical ultracentrifugation.

Light scattering analysis. Dynamic light scattering was used as a complementary method to estimate the apparent molecular masses of MBP107 and MBPstop. This technique measures the translational diffusion coefficient of polypeptides, from which the hydrodynamic (Stokes) radius can be calculated. For these proteins, data from three to five independent determinations were best fitted to either monomodal or bimodal Gaussian distributions, depending on the number of components detectable in the sample (Table 2).

The MBP107 sample contained a predominant species of 189 kDa that represented the vast majority (>99%) of the sample composition and corresponded to a tetrameric form. In contrast, MBPstop was present as a single monomeric species

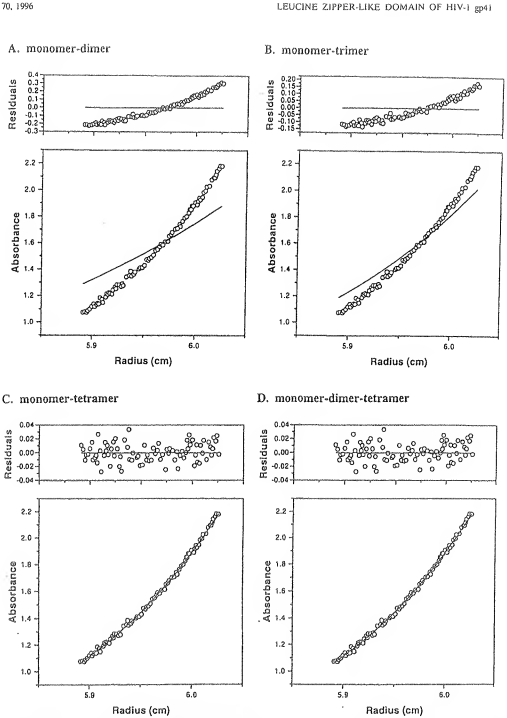

FIG. 4. Sedimentation equilibrium ultracentrifugation of MBP107 as modeled by self-associating monomer-multimer models. The concentration profile of MBP107 was obtained at 20°C and 7,000 rpm under equilibrium conditions, with an initial concentration of 1.5 mg/ml. Data were fitted to the following monomer-multimer models: monomer-dimer (fit, $\chi^2 = 2.7 \times 10^{-3}$) (A), monomer-trimer (fit, $\chi^2 = 8.4 \times 10^{-3}$) (B), monomer-tetramer (fit, $\chi^2 = 1.3 \times 10^{-4}$) (C), and monomer-dimer-tetramer (fit, $\chi^2 = 1.4 \times 10^{-4}$) (D). In each panel, the distribution of fit residuals is shown at the top and the data (plotted as solute absorbance versus radial distance) fitted to the theoretical curve (solid line) are shown at the bottom. Circles denote individual datum points. Sedimentation is from left to right.

with an apparent molecular mass of 41.4 kDa. These results are in good agreement with those obtained from analytical ultracentrifugation and size exclusion chromatography.

Chemical cross-linking analysis. To further demonstrate its oligomeric form, MBP107 was treated with the irreversible chemical cross-linker EGS, and the products were resolved by SDS-PAGE (Fig. 6). The results suggest the presence of four major species at the lowest cross-linker concentration (lane C), with an apparent molecular size of the largest form (208,000 Da) consistent with a tetramer. At the highest level of cross-linker, the tetrameric form predominates the electrophoretic profile, with little evidence for monomeric or intermediate complexes (lane F). This result is consistent with the earlier experiments and indicates that the major oligomeric species of MBP107 is tetrameric.

Antiretroviral activity. To determine whether the recombinant proteins exhibited antiviral activity, these proteins were evaluated in a HIV-1-mediated cell fusion assay (52). Since the gp41-derived sequences in these proteins are 11 residues longer than the 38-residue DP-107 peptide sequence (Fig. 1), peptides corresponding to the 49-residue gp41-specific sequences of the recombinant proteins were also synthesized and evaluated to confirm the antiviral activity of each of these slightly longer peptide sequences.

As summarized in Table 3, none of the fusion proteins inhibited syncytium formation in the cell fusion assay when assessed at the highest concentrations tested. However, both the wild-type peptide DP-280 and the parent peptide DP-107 inhibited 90% of syncytium formation at 8 μg/ml (1.4 M) and 7 μg/ml (1.6 μM), respectively. The alanine-containing peptide DP-291 also demonstrated inhibitory activity, while the serine-containing peptide DP-290 failed to exhibit antiviral activity at the highest concentration tested. These results are consistent with previously published results obtained with the shorter DP-107 peptide and related analogs (51, 52) and demonstrate the inhibitory activity of the slightly longer peptides whose gp41-derived sequences are represented in the recombinant proteins.

As shown in Table 3, the MBP107 and MBPAla proteins lacked biological activity in the cell fusion assay. Although the reason for this is unclear, the results were not unexpected since the MBP carrier represents approximately 90% of the total protein mass and may sterically hinder the accessibility of the gp41 region for its target site. Preliminary attempts to cleave the wild-type gp41-derived polypeptide from the MBP carrier by using factor Xa have resulted in only 5 to 10% effective cleavage (unpublished observations). Other investigators have also reported difficulties in cleaving MBP-based recombinant proteins with factor Xa (42). Further experiments will be required to optimize the conditions under which complete factor Xa cleavage occurs. These conditions will most likely require modification of the spacer region to a less structured sequence (42) and denaturation as the cleaved polypeptide appears to reassociate with the analogous region on intact fusion proteins (unpublished observations).

DISCUSSION

In a previous study, we reported that synthetic peptide models of the predicted gp41 leucine zipper sequence assumed a coiled-coil oligomeric structure in isotonic saline at neutral pH (52). The prototype peptide, DP-107, contained 38 residues and four heptad repeat units of the putative leucine zipper motif. As analyzed by circular dichroism, the peptide model (10 μM) adopted a stable structure which exhibited approximately 85% helicity and had a melting temperature of approximately 72°C. The melting temperature was also dependent on peptide concentration, suggesting that the helices were stabilized by association of peptide subunits to form coiled-coil oligomers, consistent with peptide models of an unrelated leucine zipper motif (34). Nevertheless, we were unable to define the exact oligomeric state determined by the gp41 zipper motif with the synthetic peptide mimics, although a recent study by Rabenstein and Shin concluded from sedimentation equilibrium experiments that DP-107 existed as a tetramer (41). In the current study, we have attempted to resolve this question by using recombinant proteins engineered to contain the gp41 zipper sequence at their C termini, reasoning that such larger proteins would be more amenable to size analysis by the physical techniques used here. Moreover, such reagents serve as a more rigorous test of the potential of the gp41 zipper domain to orchestrate oligomerization of structures with considerably more protein mass than the shorter synthetic peptides studied earlier.

Recently, Bernstein and colleagues (1) reported a similar approach in which the leucine zipper motif was expressed at the C terminus of a staphylococcal protein A (SpA) fusion protein. It was clearly demonstrated in this latter study that the gp41 heptad repeat sequence directed stable oligomerization of the SpA fusion protein as either a trimer or tetramer. A more precise definition of the multimeric state was not possible because of the asymmetry of SpA. In contrast, MBP is known to assume a spherical structure in solution (47). In agreement with these predictions, the MBP control protein (MBPstop) yielded size estimates close to theoretical by each of the techniques used (Tables 1 and 2, Fig. 5, and data not shown). The more ideal behavior of MBP then raises confidence in the molecular weight estimates of MBP-based fusion proteins that

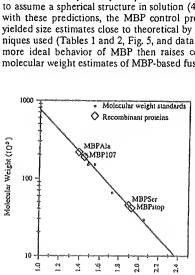

Fusion protein	Average Ve/Vo	Average molecular weight
MBP107	1.43 +/- 0.025	186,840 +/- 15,020
MBPstop	1.92 +/- 0.010	41,480 +/- 2,160
MBPAla	1.40 +/- 0.014	216,560 +/- 6,560
MBPSer	1.89 +/- 0.017	45,350 +/- 1,960

FIG. 5. Molecular weight determinations by size exclusion FPLC. A molecular weight calibration curve was obtained from the elution profiles of the following protein standards: β-amylase (200 kDa), human gamma globulin (156 kDa), alcohol dehydrogenase (150 kDa), murine immunoglobulin G2b (150 kDa), bovine serum albumin (66 kDa), and carbonic anhydrase (29 kDa). Apparent molecular weights of the fusion proteins were determined by comparing their averaged V_e/V_o ratios (obtained from four independent determinations for each fusion protein) against the calibration curve. Numerical values of the average V_e/V_o ratio, estimated molecular weights, and standard deviations are also presented.

TABLE 2. Light scattering analysis of MBP107 and MBPstop

Sample	Sample component(s)[a] (%)	Avg radius[b] (nm)	Apparent molecular mass (kDa)[c]	Predicted oligomeric state[d]
MBP107	1 (99.7)	5.59	189	Tetramer (192.7 kDa[e])
	2 (0.3)	19.15	3,763	Aggregate
MBPstop	1 (100)	2.94	41.4	Monomer (42.6 kDa)

[a] Calculated from the relative amplitude of light scattered from each component.
[b] Hydrodynamic radius of each component estimated from three to five independent determinations at room temperature, using a DynaPro-801 light scattering instrument.
[c] Estimated from the hydrodynamic radius.
[d] Predicted from the apparent molecular mass. Theoretical molecular masses are given in parentheses.

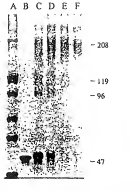

FIG. 6. SDS-PAGE analysis of cross-linked MBP107. The MBP107 fusion protein was treated for 1 h at 0°C with the cross-linker EGS at final concentrations of 0 (lane B), 0.5 mM (lane C), 1 mM (lane D), 2 mM (lane E), and 5 mM (lane F). The samples were disrupted with SDS and analyzed on an SDS-6% polyacrylamide gel. The molecular weights of standards (lane A) are shown in thousands at the left; the apparent molecular weights of the major cross-linked species are indicated in thousands at the right.

contain the wild-type gp41 heptad repeat (MBP107). As described in this report, characterization of MBP107 yielded molecular weight values consistent with tetrameric structures by all techniques used. This protein appeared to be monodisperse, with little or no evidence of monomeric, dimeric, or trimeric intermediates. This finding is consistent with the very high $K_{a1,4}$ values as estimated by sedimentation equilibrium, which predicts monomer-to-tetramer ratios of only 1 to approximately 8,000 at the concentrations studied. Similar and even higher equilibrium constants were obtained by Rabenstein and Shin for the DP-107 peptide model (41). If monomer or dimer intermediates were present, then they would be below the limits of detection associated with these techniques. The results strongly argue that the gp41 heptad repeat sequence self-associates into extremely stable tetramers which can best be defined according to a tetrameric coiled-coil structure.

Previous studies have demonstrated that multimerization events mediated through the gp41 zipper motif are critical for virus entry but not for Env assembly into oligomeric complexes (10, 11, 18, 51, 52). The lack of involvement of this region in oligomerization of the native envelope was initially puzzling given the stable multimeric structures assumed by the peptide models. This apparent anomaly is further amplified in view of the results presented in this report and those of Bernstein et al. (1) which demonstrate that the heptad repeat sequence of the gp41 ectodomain is sufficient to direct the stable oligomerization of large and otherwise monomeric proteins such as SpA and MBP. One model that reconciles these various findings is based on structural transitions in the analogous envelope component of the transmembrane envelope glycoprotein (HA2) of influenza virus. Carr and Kim (7) and Bullough et al. (6) have recently shown that a region in HA2 (residues 55 to 76 [6]) which does not participate in the trimeric coiled-coil stem structure in the native envelope state undergoes a structural rearrangement to a coiled-coil oligomer under conditions associated with membrane fusion. This site on HA2 is approximately 20 residues C terminal to the HA2 fusion peptide sequence, which is the same relative position as the gp41 heptad repeat and fusion peptide sequences (Fig. 1) (31). In an earlier report (51), we also argued that the gp41 zipper domain exists in more than one configuration during the virus life cycle. During the assembly and native states of HIV-1 Env, this region of gp41 is probably not a coiled coil but rather an undefined structure in which the individual heptad repeat sequences are held apart, perhaps through interactions with gp120 or other regions of gp41 (9). This hypothesis is consistent with both mutational experiments which suggest no role of the gp41 zipper in the oligomerization events that occur during Env assembly (11, 18, 51, 52) and deletion experiments that point to sites C terminal to the zipper region as playing the major role in Env assembly oligomerization (20). Therefore, reorientation of the heptad repeat sequences into stable coiled coils as noted here most likely occurs as an obligate step associated with membrane fusion.

Since our experiments strongly suggest a tetrameric structure for the gp41 zipper-like domain, we also believe it possible that gp41 as a whole is a tetramer in its fusion-competent state. However, there is good evidence that the HIV-1 Env precursor gp160 exists as a dimer shortly after its synthesis and during transport to the cell surface (19, 21, 39, 49). Again, the gp41 zipper region does not appear to contribute to formation of this early complex (11, 18, 49, 50). The oligomeric status of the native Env following cleavage to gp120 and gp41 is not as certain, as dimeric (19, 39, 49), trimeric (25, 35, 37), and tetrameric (19, 37, 39, 40, 45, 49) forms have been reported. Nevertheless, it is interesting to speculate that the oligomeric state of HIV-1 Env is not constant throughout the virus life cycle. Rather, Env may best be represented as a dimer during early morphogenesis steps and perhaps even in the native state but as a higher-order oligomer in the fusogenic state, the state

TABLE 3. Test for inhibition of virus-induced cell fusion

Test protein or peptide	Inhibitory concn[a]	
	μg/ml	μM
Recombinant proteins		
MBP107	>500[b]	>10.4
MBPstop	>188[b]	>4.4
MBPAla	>300[b]	>6.2
MBPSer	>280[b]	>5.8
Synthetic peptides		
DP-280 (1-578)	8	1.4
DP-291 (1-578A)	16	2.8
DP-290 (1-578S)	>50[b]	>8.8
DP-107	7	1.6

[a] Concentration of protein or peptide that gave a 90% reduction in syncytium formation between uninfected Molt-4 and HIV-1_{IIIB}-infected CEM cells.
[b] Highest concentration tested.

in which the heptad repeat coiled-coil oligomer is most likely formed (11, 18, 51, 52). Such a situation would thus be more complicated than that for the influenza virus model, which involves trimeric forms in each of the assembly, native, and fusogenic configurations of HA2 (6, 7, 53). Experiments are in progress to further address these questions and better define the oligomeric status of the DP-107 coiled-coil region as it exists within gp41 rather than as isolated heptad repeats.

Several consequences may occur as a result of gp41 heptad-mediated oligomerization during virus entry. As has been proposed for influenza virus HA2, coiled-coil formation may result in the release of the N-terminal fusion peptide sequence for subsequent insertion into the target membrane (53), the recruitment of neighboring gp41 molecules into a growing fusion pore (46), and/or the close apposition of viral and cellular membranes (55). More recent studies also suggest that the heptad repeat region defined by DP-107 may be directly involved in binding to the host cell membrane (41). The recombinant proteins described in this study should prove valuable as reagents in defining the contribution of the gp41 zipper region to the complex entry process. Independent of issues related to HIV-1 Env structure and function, the results shown here clearly demonstrate that the leucine zipper motif of gp41 can be combined with other protein sequences to yield very stable and homogeneous tetrameric chimeras. Such complexes might be of interest in a number of applications in which it is desirable to increase the valency and avidity of various proteins.

ACKNOWLEDGMENTS

We thank Gene Merutka (Trimeris Inc.) and Don McRorie (Beckman Instruments Inc.) for helpful discussions, Gene Merutka for assistance with sedimentation equilibrium experiments, and Trimeris Inc. for the use of the XL-A ultracentrifuge. We also thank Susie Farmer, Marcia Ruland, and Larry Stoltenberg for technical assistance.

D.C.S. was supported by Neurobehavioral Science Research Training Grant T32MH15177. C.T.W. is a scholar of The American Foundation for AIDS Research (AmFar grant 70036-14-RF). Additional support was provided by NIAID grant 5-R01-AI30411 and CFAR grant 5-P30-AI28662, both to T.J.M.

REFERENCES

1. Bernstein, H. B., S. P. Tucker, S. R. Kar, S. A. McPherson, D. T. McPherson, J. W. Dubay, J. Lebowitz, R. W. Compans, and E. Hunter. 1995. Oligomerization of the hydrophobic heptad repeat of gp41. J. Virol. 69:2745–2750.
2. Blondel, A., and H. Bedouelle. 1990. Expression and purification of a cytoplasmic dimeric protein by fusion to the maltose-binding protein of *Escherichia coli*. Eur. J. Biochem. 193:325–330.
3. Britton, P. 1991. Coronavirus motif. Nature (London) 353:394.
4. Buckland, R., E. Malvoisin, P. Beauverger, and F. Wild. 1992. A leucine zipper structure present in the measles virus fusion protein is not required for its tetramerization but is essential for fusion. J. Gen. Virol. 73:1703–1707.
5. Buckland, R., and F. Wild. 1989. Leucine zipper extends. Nature (London) 338:547.
6. Bullough, P. A., F. M. Hughson, J. J. Skehel, and D. C. Wiley. 1994. Structure of influenza haemagglutinin at the pH of membrane fusion. Nature (London) 371:37–43.
7. Carr, C. M., and P. S. Kim. 1993. A spring-loaded mechanism for the conformational change of influenza hemagglutinin. Cell 73:823–832.
8. Chambers, P., C. R. Pringle, and A. J. Easton. 1990. Heptad repeat sequences are located adjacent to hydrophobic regions in several types of virus fusion glycoproteins. J. Gen. Virol. 71:3075–3080.
9. Chen, C.-H., T. J. Matthews, C. B. McDanal, D. P. Bolognesi, and M. L. Greenberg. 1995. A molecular clasp in the human immunodeficiency virus (HIV) type 1 TM protein determines the anti-HIV activity of gp41 derivatives: implications for viral fusion. J. Virol. 69:3771–3777.
10. Chen, S. S.-L. 1994. Functional role of the zipper motif region of human immunodeficiency virus type 1 transmembrane protein gp41. J. Virol. 68: 2002–2010.
11. Chen, S. S.-L., C.-N. Lee, W.-R. Lee, K. McIntosh, and T.-H. Lee. 1993. Mutational analysis of the leucine zipper-like motif of the human immunodeficiency virus type 1 envelope transmembrane glycoprotein. J. Virol. 67:3615–3619.
12. Cohen, C., and D. A. D. Parry. 1986. α-helical coiled coils-a widespread motif in proteins. Trends Biol. Sci. 11:245–248.
13. Crick, F. H. C. 1953. The packing of α-helices: simple coiled coils. Acta Crystallogr. 6:689–697.
14. Crowl, R., K. Ganguly, M. Gordon, R. Conroy, M. Schaber, R. Kramer, G. Shaw, F. Wong-Staal, and E. P. Reddy. 1985. HTLV-III env gene products synthesized in *E. coli* are recognized by antibodies present in the sera of AIDS patients. Cell 41:979–986.
15. Delwart, E. L., and G. Mosialos. 1990. Retroviral envelope glycoproteins contain a "leucine zipper"-like repeat. AIDS Res. Hum. Retroviruses 6:703–706.
16. Dewar, R. L., M. B. Vasudevachari, V. Natarjan, and N. P. Salzman. 1989. Biosynthesis and processing of human immunodeficiency virus type 1 envelope glycoproteins: effects of monensin on glycosylation and transport. J. Virol. 63:2452–2456.
17. Doms, R. W., R. A. Lamb, J. K. Rose, and A. Helenius. 1993. Folding and assembly of viral membrane proteins. Virology 193:545–562.
18. Dubay, J. W., S. J. Roberts, B. Brody, and E. Hunter. 1992. Mutations in the leucine zipper of the human immunodeficiency virus type 1 transmembrane glycoprotein affect fusion and infectivity. J. Virol. 66:4748–4756.
19. Earl, P. L., R. W. Doms, and B. Moss. 1990. Oligomeric structure of the human immunodeficiency virus type 1 envelope glycoprotein. Proc. Natl. Acad. Sci. USA 87:648–652.
20. Earl, P. L., and B. Moss. 1993. Mutational analysis of the assembly domain of the HIV-1 envelope glycoprotein. AIDS Res. Hum. Retroviruses 9:589–594.
21. Earl, P. L., B. Moss, and R. W. Doms. 1991. Folding, interaction with GRP78-BiP, assembly, and transport of the human immunodeficiency virus type 1 envelope protein. J. Virol. 65:2047–2055.
22. Edelhoch, H. 1967. Spectroscopic determination of tryptophan and tyrosine in proteins. Biochemistry 6:1948–1954.
23. Ellenberger, T. E., C. J. Brandl, K. Struhl, and S. C. Harrison. 1992. The GCN4 basic region leucine zipper binds DNA as a dimer of uninterrupted α-helices: crystal structure of the protein-DNA complex. Cell 71:1223–1237.
24. Gallaher, W. R., J. M. Ball, R. F. Garry, M. C. Griffin, and R. C. Montelaro. 1989. A general model for the transmembrane proteins of HIV and other retroviruses. AIDS Res. Hum. Retroviruses 5:431–440
25. Gelderblom, H. R., E. H. S. Hausmann, M. Ozel, G. Pauli, and M. A. Koch. 1987. Fine structure of human immunodeficiency virus (HIV) and immunolocalization of structural proteins. Virology 156:171–176.
26. Gonn, C., P. Li, P. D. Riggs, and H. Inouye. 1987. Vectors that facilitate the expression and purification of foreign peptides in *Escherichia coli* by fusion to maltose-binding protein. Gene 67:21–30.
27. Ho, S. N., H. D. Hunt, R. M. Horton, J. K. Pullen, and L. R. Pease. 1989. Site-directed mutagenesis by overlap extension using the polymerase chain reaction. Gene 77:51–59.
28. Landschulz, W. H., P. F. Johnson, and S. L. McKnight. 1988. The leucine zipper: a hypothetical structure common to a new class of DNA binding proteins. Science 240:1759–1764.
29. Laue, T. M., B. D. Shah, T. M. Ridgeway, and S. L. Pelletier. 1992. Computer-aided interpretation of analytical sedimentation data for proteins, p. 90–125. *In* S. E. Harding, A. J. Rowe, and J. C. Horton (ed.), Analytical ultracentrifugation in biochemistry and polymer science. The Royal Society of Chemistry, Cambridge.
30. Mellins, M. H., J. Reuber, R. Fenrick, and B. R. Cullen. 1988. Immunodeficiency virus *rev trans*-activator modulates the expression of the viral regulatory genes. Nature (London) 335:181–183.
31. Myers, G., B. Korber, S. Wain-Hobson, R. F. Smith, and G. N. Pavlakis. 1993. Human retroviruses and AIDS 1993 I-II: a compilation and analysis of nucleic acid and amino acid sequences. Los Alamos National Laboratory. Los Alamos, N. Mex.
32. Nagia, K., and H. C. Thogersen. 1987. Synthesis and sequence-specific proteolysis of hybrid proteins produced in *Escherichia coli*. Methods Enzymol. 153:461–481.
33. O'Shea, E. K., J. D. Klemm, P. S. Kim, and T. Alber. 1991. X-ray structure of the GCN4 leucine zipper, a two-stranded, parallel coiled coil. Science 254:539–544.
34. O'Shea, E. K., R. Rutkowski, and P. S. Kim. 1989. Evidence that the leucine zipper is a coiled coil. Science 243:538–542.
35. Owens, R. J., and R. W. Compans. 1990. The human immunodeficiency virus type 1 envelope glycoprotein precursor acquires aberrant intermolecular disulfide bonds that may prevent normal proteolytic processing. Virology 179:827–833.
36. Peteranderl, R., and H. C. M. Nelson. 1992. Trimerization of the heat shock transcription factor by a triple-stranded α-helical coiled-coil. Biochemistry 31:12272–12276.
37. Pinter, A., W. J. Honnen, S. A. Tilley, C. Bona, H. Zaghouani, M. K. Gorny, and S. Zolla-Pazner. 1989. Oligomeric structure of gp41, the transmembrane protein of human immunodeficiency virus type 1. J. Virol. 63:2674–2679.
38. Popovic, M., M. G. Sarngadharan, E. Read, and R. C. Gallo. 1984. Detection, isolation and continuous production of cytopathic retroviruses (HTLV-III) from patients with AIDS and pre-AIDS. Science 224:497–500.